Micro and nano-indentation of $MoSi_2$

M. HENŽEL, J. KOVALČÍK, J. DUSZA*
Department of Structural Ceramics, Institute of Materials Research of the Slovak Academy of Sciences, Watsonova 47, 04353 Košice, Slovakia
E-mail: dusza@imrnov.saske.sk

A. JUHÁSZ, J. LENDVAI
Department of General Physics, ELTE, Pázmány Péter sétány 1/A, 1117 Budapest, Hungary

Molybdenum disilicide based materials are candidate for high temperature structural applications, such as a furnace heating element and an electrical conductor in silicon intergrated circuit design or parts of engines [1]. $MoSi_2$ exhibits a high melting point (2030 °C), excellent high temperature oxidation resistance, and posseses many convenient properties such as high stiffness, high thermal conductivity, relatively low density, and high strength at elevated temperatures. However, a major difficulty in application of these materials is the lack of adequate ductility and fracture toughness below 1000 °C. Only toward the higher temperatures (between 1000 and 1400 °C), with the onset of dislocation climb and diffusional creep processes, does $MoSi_2$ exhibit significant plasticity in compression, bending, and tension in both single crystals and polycrystalline materials [2, 3]. During the last decade many approaches had been applied to reduce the brittle-to-ductile transition temperature (BDTT) of these materials, to overcome the limitation of dislocation mobility and dislocation density, and to enhance the capability for plastic flow and increase the fracture toughness. The main approaches for ductility enhancement are solid solution alloying, second phase microstructure control, ductile phase toughening, and high temperature prestrain [4].

The crystal structure of $MoSi_2$ is tetragonal (C11b type), space group $14/mmm$. The lattice parameters are $a = 0.3205$ nm and $c = 0.7845$ nm with $c/a = 2.45$ (Fig. 1). $MoSi_2$ is also reported to have hexagonal C40 structure above 1900 °C [5]. There exists an absence of knowledge concerning the relative mobility of edge and screw dislocations and information about different dislocation types $\langle 100 \rangle$, $\langle 110 \rangle$, $1/2\langle 111 \rangle$, and $1/2\langle 331 \rangle$, their glide planes; furthermore the operative slip systems as a function of temperature, strain rate, and crystallographic orientation are only partially understood. Studies of the slip systems by means of hardness indentation for $MoSi_2$ single crystal has found that the primary and secondary slip systems were $\{100\}\ \langle 001 \rangle$ and $\{110\}\ \langle 001 \rangle$, respectively [4]. Berkowitz *et al.* [6] reported that {110} is the slip plane in $MoSi_2$ single crystal deformed between 625 and 1125 °C under compressive load along three different directions. They concluded that the slip direction is $\langle 1\bar{1}0 \rangle$. Umakoshi *et al.* [7] reported that slip occurs in $\langle \bar{3}30 \rangle$ directions on both {110} and {103} planes.

Newly developed materials are often prepared in limited quantities and shapes unsuitable for extensive mechanical testing. Development of depth sensing indentation methods introduced the advantage of load and depth measurement during the indentation cycle [8]. This enables, by using a simple and fast measurement, to evaluate not only hardness, for which the indentation is traditionally used, but also elastic modulus, yield behaviour, plasticity, the onset of other irreversible deformation processes—such as cracking or pressure induced phase transformations, time-dependent phenomena—such as creep and recovery, and the energy absorbed during indentation. These problems can be studied on very small samples, with high spatial resolution, and non-destructively, if necessary [9].

The aim of this contribution is to study the micro/nano hardness of an as-received and as-deformed $MoSi_2$ in order to compare the hardness values measured by different methods and to study the influence of pre-strain on the micro/nano hardness.

The material used in this investigation was monolithic $MoSi_2$ prepared by Cesiwid, Erlangen, Germany. Samples for microstructure analysis were prepared using standard procedure and investigated using optical microscopy, as well as scanning and transmission electron microscopy (SEM and TEM). The pre-strain was performed by compressive creep test at the applied load of 15 MPa at 1400 °C for 24 hr.

Mirror polished samples prepared by conventional ceramography have been used for hardness tests. The depth sensing tests were performed with Shimadzu DUH device with Vickers indenter. Nominal peak loads of 10 to 2000 mN were used and the dwell time at maximum load was 10 s. Measurement of conventional hardness was carried out using Leco LM700AT microhardness tester with loads of 500, 1000, and 2000 mN, with a dwell time of 10 s.

The universal hardness is defined as the test force (load) F divided by the apparent area of the indentation $A(h)$ under the applied test force and can be calculated

*Author to whom all correspondence should be addressed.

0022–2461

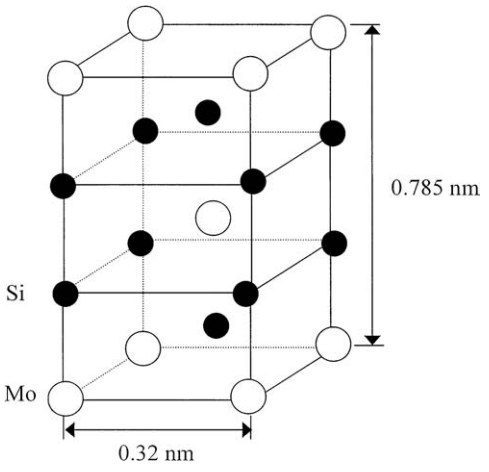

Figure 1 Tetragonal unit cell of $MoSi_2$.

from the following equation [10]:

$$\mathrm{HU} = F/26.43\,h^2 \tag{1}$$

where F is the applied load in N and h is the indentation depth in mm.

The plastic hardness is the quotient from the test force divided by an area calculated by the extrapolation:

$$\mathrm{HU_{plast}} = F_{\max}/26.43\,h_r^2 \tag{2}$$

where $F_{\max}$ is the maximum force (load) in N and h_r is the indentation depth resulting as the intersection of the tangent of indentation depth curve at the maximum force (range of the removal of test force) with the indentation depth axis in mm.

With the known Young's modulus of the tested material, an analytic solution separates the contribution of elastic deformation, converting HU into the conventional hardness HV, which is related to the plastic indent size. HV is calculated from the following equation:

$$\mathrm{HU_{plast}} = 4\mathrm{HU}/\{1 + \sqrt{(1 - 12\mathrm{HU}/E^*)}\}^2 \tag{3}$$

where E^* is the effective contact stiffness, which can be determined from the equation [11]

$$E^* = \left\{\left(1 - \nu_s^2\right)/E_s + \left(1 - \nu_i^2\right)/E_i\right\}^{-1} \tag{4}$$

where E_i is Young's modulus of the indenter, ν_i is Poisson's ratio of the indenter, E_s is Young's modulus of the tested material, and ν_s is Poisson's ratio of the tested material.

The conventional Vickers hardness is calculated from the equation

$$\mathrm{HV} = 1.8544F/a^2 \tag{5}$$

where F is the applied force (load) in kg and a is the diagonal of the indentation in mm.

The microstructure of the studied material is shown in Fig. 2. Using SEM and EDX it was found that there were three different phases present in the microstructure of the monolithic $MoSi_2$:$MoSi_2$ matrix grains, SiO_2, and a little Mo_5Si_3 (hexagonal Nowotny phase).

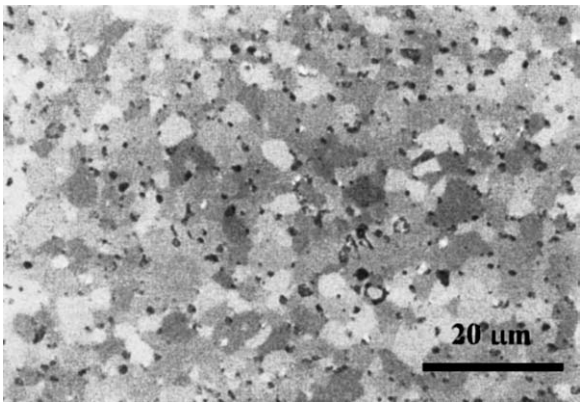

Figure 2 Microstructure of $MoSi_2$.

Figs 3 and 4 present different F–h curves obtained for the $MoSi_2$ intermetallics under study. Values of the universal hardness and plastic hardness are recorded in the same figure. The approximate value of hardness can be taken from the steady-state curve of universal and plastic hardness. Values of the universal and plastic hardness taken from the steady-state curves are presented in Table I. Values of the conventional Vickers hardness are presented in Table II.

Both universal and conventional hardness exhibit obvious load size effect; the hardness increases with decreasing indentation depth. Similar load size effect has been found in many ceramics, but also in $MoSi_2$ [12–14]. Boldt *et al.* [13] investigated microhardness of a $MoSi_2$ single crystal using Vickers indentation with loads from 50 to 14 000 mN. A constant hardness of approximately 10 GPa was found until the applied load has been reduced to approximately 2000 mN. At this point the hardness values begin to increase toward a value of 19 GPa at the 50 mN load. Morris *et al.* [14] studied the conventional Vickers microhardness of a monolithic, reactive sintered polycrystalline $MoSi_2$ at loads from 500 to 1000 mN. Microhardness values of the materials changed from 12.4 to 14.3 GPa in dependence on the sintering temperature. These results

TABLE I Hardness values calculated from the $-P$–h curves

Max. load (mN)	Microhardness (GPa)			
	As-received state		As-deformed state	
	HU	$\mathrm{HU_{plast}}$	HU	$\mathrm{HU_{plast}}$
500	7.66	9.19	5.51	6.25
50	10.78	14.17	9.35	11.77

TABLE II Traditional Vickers microhardness values

Max. load (mN)	Microhardness (GPa)	
	As-received state	As-deformed state
	HV	HV
500	13.34	11.78
1000	11.27	10.04
2000	10.84	10.44

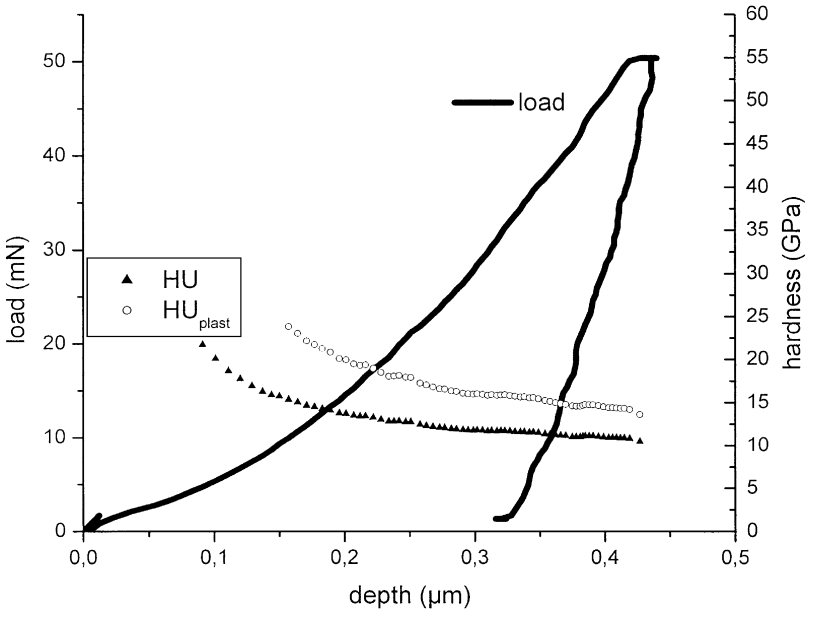

Figure 3 Depth-sensing curve of the as-received state with the maximum load of 50 mN.

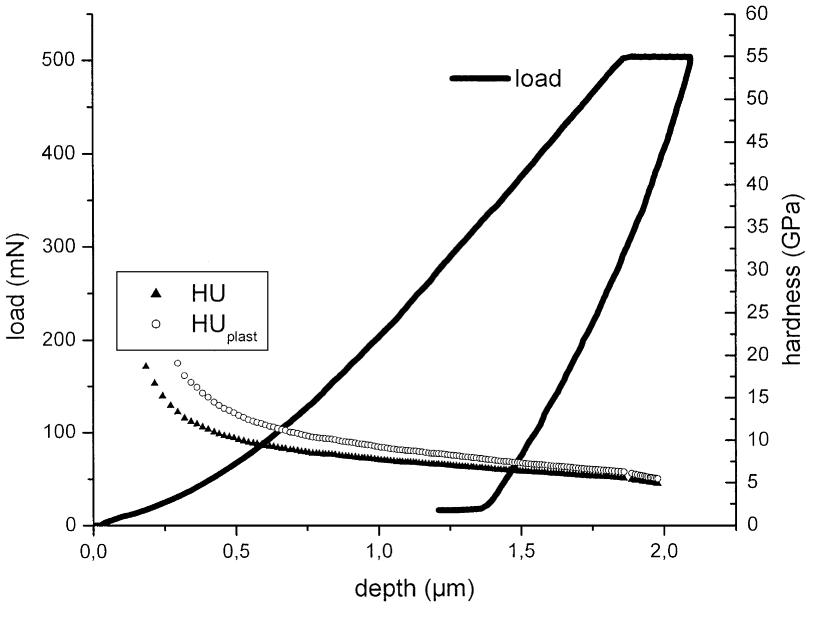

Figure 4 Depth-sensing curve of the as-deformed state with the maximum load of 500 mN.

are in full agreement with our results achieved on the as-received material.

Ullmer *et al*. [15] compared the instrumented and conventional hardness tests for testing different advanced ceramics. There does not exist a systematic relationship between the conventional Vickers and plastic hardness of the tested materials. The plastic hardness corresponds with the conventional Vickers hardness for specimens qualified for reference materials only, and both hardness values become significantly different for commercial engineering materials with higher porosity.

In Figs 5 and 6 shapes of the P–h curves are illustrated for the as-received and as-deformed materials at the maximum load of 500 and 50 mN, respectively. Differences in the shape of P–h curves in the as-received and as-deformed materials demonstrates that the as-deformed material has a higher deformation ability and is softer when compared with the as-received one. Such behaviour is more evident when tested at the maximum load of 500 mN. Similar behaviour has been recognized also during the conventional Vickers hardness test, but the difference between the hardness of the as-received and as-deformed materials is significantly lower. It can be explained by the presence of slip systems in the as-deformed material being activated during the pre-strain procedure. To verify this assumption additional experiments have to be performed.

A distinct indentation load size effect was found for the universal, plastic, and conventional Vickers hardness of the as-received and as-deformed $MoSi_2$. The plastic hardness was lower in comparison to the conventional Vickers hardness for both materials and at all indentation loads. The pre-strain can change deformation ability and hardness of the $MoSi_2$ even at room temperature.

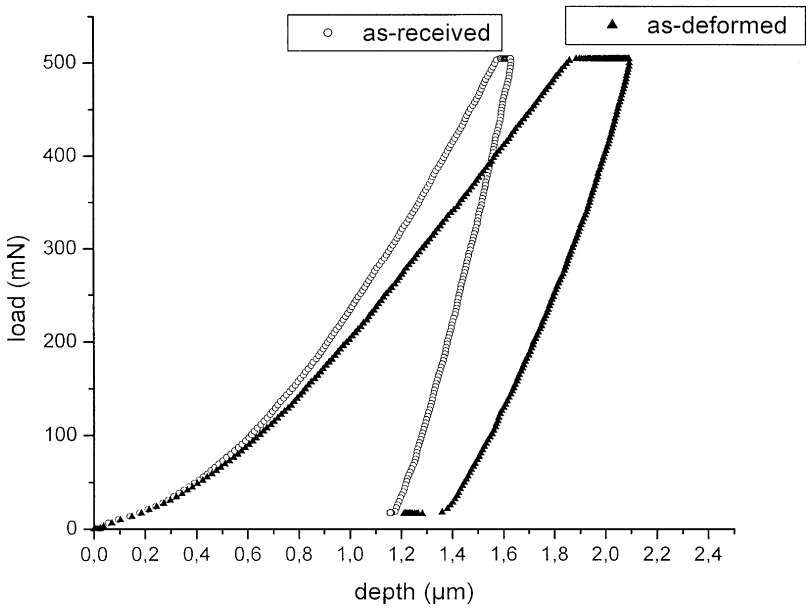

Figure 5 Comparisons of the *P–h* curves for the as-received and as-deformated states with the maximum load of 500 mN.

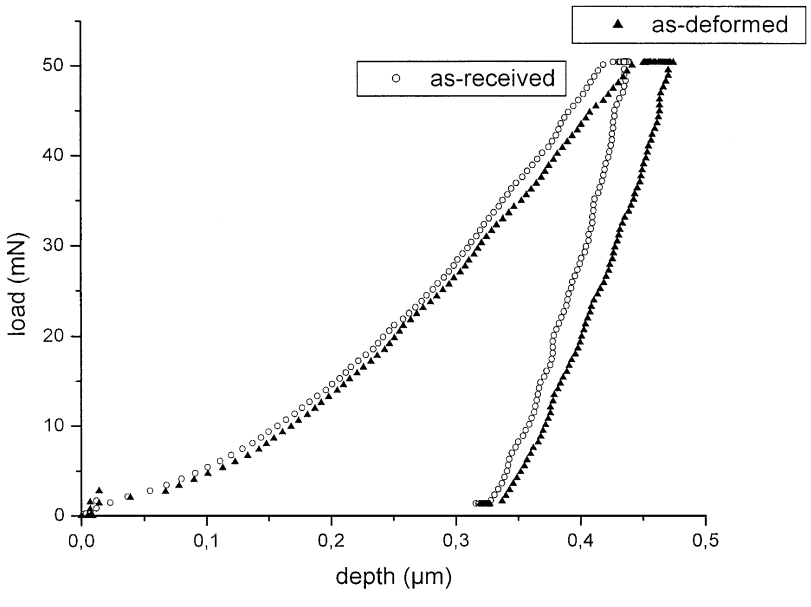

Figure 6 Comparisons of the *P–h* curves for the as-received and as-deformated states with the maximum load of 50 mN.

Acknowledgments

This work was realized with the financial support of the Slovak Grant Agency, under the contract No. 2/1166/21 and by NANOSMART, Centre of Excellence, SAS.

References

1. A. K. VASUDEVAN and J. J. PETROVIC, *Mater. Sci. Eng.* A **155** (1992) 1.
2. O. UNAL, J. J. PETROVIC, D. H. CARTER and T. E. MITCHELL, *J. Amer. Ceram. Soc.* **73** (6) (1990) 1752.
3. T. E. MITCHELL, R. G. CASTRO and J. J. PETROVIC, *Mater. Sci. Eng.* A **155** (1992) 241.
4. R. GIBALA, H. CHANG, C. M. CZARNIK and J. P. CAMPBELL, *Mater. Sci. Eng.* A **261** (1999) 122.
5. S. INOU, N. TOYOKURA, T. NAKAMURA, M. MAEDA and M. TAKAGI, *J. Electro. Soc.* **130**(7) (1983) 1603.
6. J. BERKOWITZ-MATTUCK and M. ROSSETTINASW-1887, Cambridge, MA, 1971.
7. Y. UMAKOSHI and T. SAKAGAMI *et al.*, **59**(4) (1989) 159.
8. W. C. OLIVER and G. M. PHARR *J. Mater. Res.* 7 (1992) 1564.
9. A. J. BUSHBY, Nondestructive Testing and Evaluation **17** (2001) 213.
10. DIN 20339 Universalhärteprüfung, October 1997.
11. A. KRELL and S. SCHADLICH, *Mater. Sci. Eng.* A **307** (2001) 172.
12. J. DUSZA.
13. P. H. BOLDT, J. D. EMBURRY and G. C. WEATHERLY, *Mater. Sci. Eng.* A **155** (1992) 251.
14. D. G. MORRIS, M. LEBOEUF and M. A. MORRIS, *Mater. Sci. Eng.* A **251** (1998) 262.
15. CH. ULLNER, J. BECKMANN and R. MORRELL, *J. Europ. Cer. Soc.* **22** (2002) 1183.

Received 12 September 2003
and accepted 10 February 2004